

# Spiking Neural Networks for Mental Workload Classification with a Multimodal Approach

Jiahui An<sup>\*†</sup>, Sara Irina Fabrikant<sup>‡</sup>, Giacomo Indiveri<sup>†</sup>, Elisa Donati<sup>†</sup>

<sup>\*</sup>Institute of Neuroinformatics, University of Zurich and ETH Zurich, Zurich, Switzerland

<sup>†</sup>Digital Society Initiative, University of Zurich, Zurich, Switzerland

<sup>‡</sup> Department of Geography and Digital Society Initiative, University of Zürich, Zürich, Switzerland

**Abstract**—Accurately assessing mental workload is crucial in cognitive neuroscience, human-computer interaction, and real-time monitoring, as cognitive load fluctuations affect performance and decision-making. While Electroencephalography (EEG)-based machine learning (ML) models can be used to this end, their high computational cost hinders embedded real-time applications. Hardware implementations of spiking neural networks (SNNs) offer a promising alternative for low-power, fast, event-driven processing.

This study compares hardware-compatible SNN models with various traditional ML ones, using an open-source multimodal dataset. Our results show that multimodal integration improves accuracy, with SNN performance comparable to the ML one, demonstrating their potential for real-time implementations of cognitive load detection.

These findings position event-based processing as a promising solution for low-latency, energy-efficient workload monitoring, in adaptive closed-loop embedded devices that dynamically regulate cognitive demands.

**Index Terms**—Mental workload classification, spiking neural networks, multimodal physiological signals, brain computer interface

## I. INTRODUCTION

Mental workload (also called cognitive load) refers to the mental effort or resources a person uses to perform a task, distinct from the task's external demands [1].

Mental workload classification plays a vital role in enhancing human-computer interaction, advancing cognitive neuroscience, and enabling real-time physiological monitoring. Understanding and accurately assessing cognitive load is essential for optimizing system responsiveness, improving user experience, and ensuring safety in high-stakes environments [2–5].

Traditional approaches have primarily relied on Machine Learning (ML)-based classifiers trained on brain signal datasets such as Electroencephalography (EEG) ones [1, 3, 6]. However, these models often require extensive computational resources, limiting their deployment in real-time and low-power applications [7]. Moreover, since these studies are focusing solely on EEG, they overlook the potential benefits of multimodal physiological data integration [6, 8].

In this study, we used an open-source multimodal dataset (EEG, heart rate variability, electrodermal activity, and skin temperature) [9], which was evaluated only using a Logistic

Regression (LR) model. This limitation presented an opportunity for further exploration using alternative advanced classification techniques. Therefore we developed an event-based approach that can be deployed onto neuromorphic chips to enable mental workload classification with low latency and low energy consumption. Indeed, neuromorphic computing, inspired by the efficiency of biological neural networks, offers a promising alternative to conventional ML models by leveraging Spiking Neural Networks (SNNs) for event-driven computation [7, 10].

Unlike previous studies that solely relied on EEG or other brain signals for mental workload classification, this work incorporates the analysis of EEG, heart rate variability (HRV), Electrodermal activity (EDA), and Temperature (TEMP) features. The integration of multiple physiological signals can enhance classification performance by capturing a more comprehensive representation of cognitive load variations [8, 11].

While ML-based classifiers such as Support Vector Machines (SVMs) and LR have been widely used for mental workload classification, neuromorphic approaches based on SNNs remain largely unexplored. This work addresses two key questions: (1) Can SNNs achieve performance comparable to state-of-the-art ML models in mental workload classification? (2) Are brain signals alone sufficient to detect cognitive load changes, or is a multimodal approach essential for robust classification?

For the first time, we demonstrate the use of SNN for cognitive load classification, building on previous successful results in biosignal processing. Neuromorphic architectures have demonstrated the ability to detect anomalies in Electrocardiography (ECG) recordings [12–14], classify Electromyography (EMG) signals [15–17], and identify relevant biomarkers in EEG data measured from epileptic patients [18, 19]. These findings suggest that SNNs offer a promising, biologically inspired alternative to traditional ML approaches for cognitive load monitoring [20–24].

To address these questions, we systematically compared ML-based methods with neuromorphic approaches, assessing their classification accuracy across different feature sets. Our findings offer new insights into the potential of SNNs for mental workload monitoring, laying the foundation for real-time, energy-efficient implementations in wearable and embedded

systems.

## II. METHODS

In this section, we describe our methodology for cognitive load classification using multimodal physiological signals.

### A. Data Description

This study utilized an open-source dataset containing 315 hours of multimodal physiological recordings from 24 participants [9]. Data were collected in both controlled laboratory settings and self-selected, uncontrolled environments. However, we focused solely on the controlled sessions, as they involve standardized cognitive tasks that minimize external variability, ensuring consistency across participants and improving comparability and generalizability.

The dataset includes multiple modalities. Brain signals were recorded using the Muse S EEG headband at 256 Hz from five sensor locations: AF7 and AF8 at the frontal lobe, TP9 and TP10 at the temporal lobe, and FpZ as the reference channel following the EEG 10/20 international system (e.g., a standardized method for electrode placement based on scalp proportions). Physiological signals were captured using the Empatica E4 wristband, which recorded Photoplethysmography (PPG) at 64 Hz for HRV, EDA at 4 Hz to assess autonomic nervous system responses, and temperature at 4 Hz to monitor core body fluctuations. Additionally, acceleration data were recorded at 32 Hz to account for motion-related artifacts.

Participants performed structured cognitive tasks designed to induce different levels of mental workload, including mental arithmetic, Stroop, N-back (two levels), and Sudoku. Each task lasted 10 minutes, ensuring a balanced class distribution (Easy:Hard = 50:50).

For this study, we randomly selected 10 participants with complete controlled session data to balance computational efficiency and statistical robustness. This subset provides sufficient data diversity while keeping the study focused and feasible.

### B. Preprocessing and Feature Extraction

EEG signals were bandpass-filtered between 0.5 and 50 Hz using a Butterworth filter to remove low-frequency drifts and high-frequency muscle artifacts, with an additional 50 Hz notch filter to eliminate power-line interference. Baseline normalization was performed using an eye-closing session, and signals were average-referenced. Power spectral density (PSD) was computed using Welch's method for five frequency bands:  $\delta$  (0.5–4 Hz),  $\theta$  (4–7 Hz),  $\alpha$  (8–12 Hz),  $\beta$  (12–30 Hz), and  $\gamma$  (30–50 Hz). Asymmetry features were derived by subtracting the log-transformed spectral power of the right hemisphere from the left across all frequency bands. Additionally, the  $\theta/\alpha$  and  $\alpha/\theta$  ratios were computed to enhance cognitive load estimation.

HRV features were extracted from the PPG signal using the NeuroKit2 package, including: time-domain metrics – i.e. mean RR interval (HRV-MeanNN), standard deviation of RR intervals (HRV-SDNN), and root mean square of successive

differences (HRV-RMSSD) –, and frequency-domain measures – normalized low-frequency power (HRV-LFn), normalized high-frequency power (HRV-HFn), and their ratio. EDA included the number of Skin Conductance Response (SCR) peaks and their mean amplitude, while temperature features were computed as the mean and standard deviation over time.

Variance thresholding resulted in most participants (9 out of 10) retaining 23 features, while one participant (UN\_105) retained 27 features due to higher physiological signal variability. The four features removed for most participants were all related to EDA—specifically, EDA\_Tonic\_SD, EDA\_Sympathetic, EDA\_SympatheticN, and EDA\_Autocorrelation. Their removal suggests that these features exhibited low variance across participants and contributed minimally to cognitive load classification.

All signals were segmented using a 60-second sliding window with an 80% overlap to effectively capture temporal dynamics. Missing values were interpolated using the mean of neighboring values, and all features were standardized to achieve zero mean and unit variance. Each 60-second segment was labeled as “Easy” (0) or “Hard” (1) based on the difficulty level of the corresponding cognitive task.

Figure 1 provides an overview of the multimodal data acquisition setup, showing the EEG electrode placement and wearable sensors and extracted physiological signals used for cognitive load classification.

### C. Model Architecture and Training

As a baseline, we implemented a LR model with L2 regularization, optimized via grid search (over L1 and L2 penalties with solvers such as liblinear, saga and lbfgs) for each participant. The data was partitioned into an 80/20 training/testing split, with stratified 5-fold cross-validation. Compared to prior work using a similar dataset (which achieved 71% accuracy) which were comparable to our LR model (which achieved 78%). To further enhance performance, we explored more complex non-linear models, including Multilayer Perceptron (MLP), SVM (Polynomial and RBF kernels), and SNN, which are better suited for capturing complex relationships in multimodal physiological data.

1) *Models on EEG Features only:* To assess the effectiveness of EEG features alone, we trained LR, MLP, and SVM models using EEG-derived features. EEG preprocessing followed the pipeline described earlier, including standard scaling and variance threshold filtering to remove redundant features. We implemented the LR model as described in the baseline model above with EEG features only.

For MLP, we optimized the architecture and hyperparameters via grid search for each participant, which included one or two hidden layers (e.g., 50 neurons in a single layer, 100 neurons, two layers with 50 neurons each or two layers one with 50 neurons the other one with 100 neurons), Rectified Linear Unit (ReLU) or tanh activation, learning rates (0.001–0.01), and early stopping criteria.

We implemented SVM models with linear, polynomial, and Radial basis function (RBF) kernels were trained, with

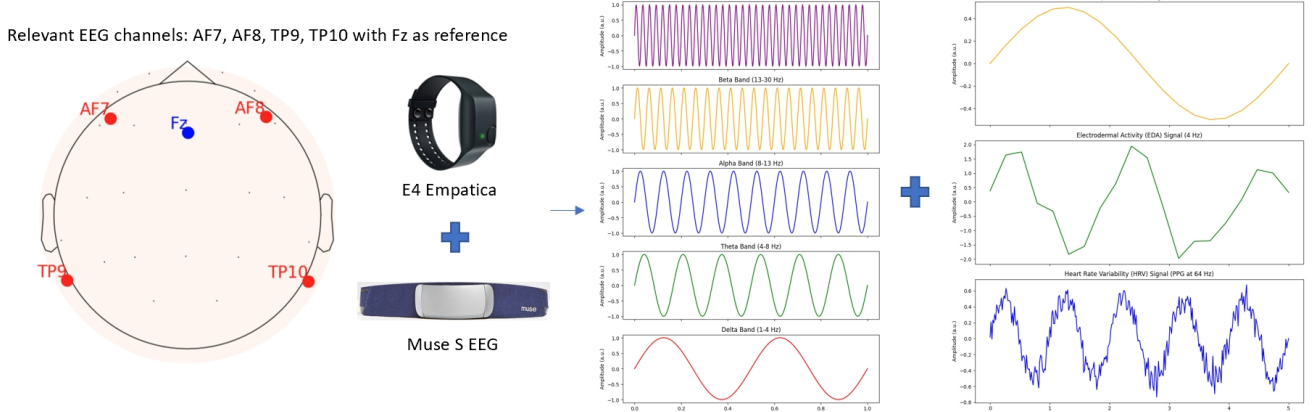


Fig. 1: Schematic representation of the multimodal data acquisition system. EEG signals were recorded using the Muse S headband at five sensor locations (AF7, AF8, TP9, TP10, and Fz as reference), while physiological signals, including heart rate variability, electrodermal activity, and temperature, were captured using the Empatica E4 wristband. The recorded physiological signals were integrated for cognitive load classification after feature extraction.

hyperparameter tuning including regularization strength  $C$ , kernel-specific parameters (degree and gamma for polynomial and RBF kernels), and class weights. These EEG-only models provided an initial benchmark before integrating multimodal physiological features.

To determine the optimal EEG feature combination for cognitive load classification, we evaluated three feature sets: (1) *Basic PSD*—including mean spectral power in five frequency bands:  $\delta$  (1–4 Hz),  $\theta$  (4–7 Hz),  $\alpha$  (8–12 Hz),  $\beta$  (12–30 Hz),  $\gamma$  (30–50 Hz); (2) *PSD + Asy*—which adds asymmetry measures (e.g., frontal- $\alpha$ -asymmetry) to the Basic PSD; and (3) *PSD + Asy + Ratios*—which further included power ratios (such as  $\theta/\alpha$  and  $\alpha/\theta$ ).

2) *Training ML-based Models with All Modalities*: With this analysis, we aim to investigate whether adding modalities improves classifier performance. LR models were optimized via grid search over regularization parameters, while MLP tuning focused on hidden layer sizes, regularization parameter  $\alpha$ , learning rate, and activation functions. SVM models retained the same tuning procedure as in EEG-only experiments but now incorporated multimodal features.

3) *Training Spiking Neural Networks*: To further explore neuromorphic approaches for cognitive load classification, we implemented multiple SNNs using a spiking version of Python [25].

Our SNNs employed forward-pass, where input features were processed through the first layer (fc1) and its associated Leaky Integrate-and-Fire (LIF) layer to produce spike outputs, which were then fed into a second LIF layer (fc2). Training follows two approaches:

a) *Hybrid SNN (Bio-Inspired + Backpropagation)*:

- The fc1 weights are updated using the Adam optimizer via standard backpropagation.
- The fc2 weights are updated using a delta learning rule, where the error is computed as the difference between the target label and the sum of output spikes:

$$\Delta W_{fc2} = \eta \cdot (S_{fc1}^\top \cdot \Delta), \quad (1)$$

where  $\eta$  is the learning rate, and  $S_{fc1}^\top$  represents the spike outputs from fc1. The error ( $\Delta$ ) is given by:

$$\Delta = y - \sum S_{\text{out}}. \quad (2)$$

Hyperparameter tuning for the network architecture was performed via grid search over the hidden layer size (set to 20 times the number of input features), learning rate (0.001, 0.01, or 0.1), number of epochs (10 or 20), and a batch size of 1, with early stopping applied after 5 epochs without improvement. We employed stratified 5-fold cross-validation for each participant to select the best hyperparameter configuration based on mean validation accuracy and applied early stopping when performance did not improve over 5 consecutive epochs. This approach—though it used backpropagation for fc1 updates—was intended for simulation with `snntorch` and served as a precursor to more biologically inspired models that would abandon backpropagation entirely for neuromorphic hardware implementation.

b) *Bio-Inspired SNN*: We then implemented a second SNN using one single layer training that allowed the implementation on a mixed analog/digital chip. We first converted the continuous input features into spikes using LIF neurons. The spike encoding was achieved using parameters that mimic biological neurons: a resting potential of 0, a reset potential of  $-65.0$ , a firing threshold of  $-50.0$ , a membrane time constant  $\tau$ , and a simulation time step of 1 ms ( $dt$ ) across 40 steps. The num\_steps which was defined by the dataset: the total recording for each participant lasted 40 minutes, and each feature was extracted based on a 1-minute recording. The  $\tau$  was optimized through grid search.

- The fc1 weights remain fixed, initialized from a normal distribution with a mean of 0.1 and a standard deviation of 0.02.

- The fc2 weights are updated via the delta learning rule.

The LIF neuron model followed the standard differential equation governing membrane potential dynamics:

$$\tau \frac{dV(t)}{dt} = -(V(t) - V_{\text{rest}}) + X(t), \quad (3)$$

where  $V(t)$  is the membrane potential at time  $t$ ,  $V_{\text{rest}}$  is the resting membrane potential, and  $\tau$  is the membrane time constant. Unlike conventional implementations, where  $I_{\text{in}}(t)$  represents an explicit input current, in this study, we define the input term  $X(t)$  as the input feature vector. This means that instead of receiving a direct synaptic current, the LIF neuron directly integrates feature values as part of its membrane dynamics.

A spike is emitted when the membrane potential reaches the threshold  $V_{\text{th}}$ , at which point the membrane potential is reset to  $V_{\text{reset}}$ :

$$V(t) = V_{\text{reset}}, \quad \text{if } V(t) \geq V_{\text{th}}. \quad (4)$$

The network architecture was similar to the previous SNN but now applied LIF neurons with a learnable beta parameter in both layers. The second layer (fc2) remained fully connected, while the first layer (fc1) introduced a connection probability parameter ( $p_{\text{conn}}$ ). The fc1 weights were initialized from a normal distribution with a mean of 0.1 and a standard deviation of 0.02 (i.e., 0.2 times the mean), following the same initialization for ( $p_{\text{conn}}$ ). The optimal mean for fc1 weights and the best ( $p_{\text{conn}}$ ) distribution were determined via grid search. A schematic representation is shown in Fig. 2.

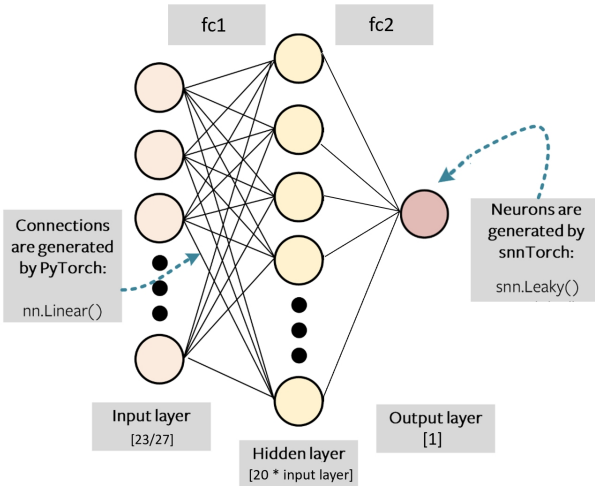


Fig. 2: Schematic representation of the SNN architecture. The model consists of two fully connected layers (fc1 and fc2) with LIF neurons. The first layer (fc1) incorporates a connection probability parameter ( $p_{\text{conn}}$ ) and learnable beta in LIF neurons, while the second layer (fc2) updates weights using a delta learning rule.

For classification, the output neuron's spiking activity is interpreted as follows: if the membrane potential reaches the threshold and a spike occurs, the network predicts Class 1; otherwise, it predicts Class 0. The output neuron follows a threshold-based activation function with a default threshold of 1.0, ensuring discrete decision-making.

Additionally, we trained the bio-inspired SNN on two different input configurations: EEG features only and all physiological modalities (EEG, HRV, EDA, TEMP).

#### D. Evaluation Metrics

Model performance was evaluated using four key metrics: accuracy, F1-score, precision, and recall. These metrics were computed on an independent 20% testing set. To account for variability across participants, all performance metrics were averaged across stratified  $k$ -fold cross-validation splits ( $k = 5$ ), providing robust estimates of classification performance.

To determine whether significant differences existed between model performances, we conducted a series of statistical tests on the classification accuracy across participants. The selection of statistical tests was based on the distribution of model accuracies.

1) *Bootstrapping Procedure*: We applied a bootstrapping procedure by generating 1000 resampled accuracy distributions for each model based on their mean and standard deviation. This resampling method enhanced statistical power and provided more reliable estimates of model performance variability. The bootstrapped distributions were then used for subsequent statistical tests.

2) *Normality Test*: Before selecting appropriate statistical tests, we assessed whether the bootstrapped accuracy distributions for each model adhered to a normal distribution using the Shapiro-Wilk test. If the normality assumption was satisfied ( $p > 0.05$ ), we proceeded with parametric statistical tests, such as one-way ANOVA or Generalized Linear Model (GLM) for multiple model comparisons. If the normality assumption was violated ( $p \leq 0.05$ ), we opted for non-parametric alternatives, including Kruskal-Wallis test and Wilcoxon Signed-Rank test.

3) *Multiple Model Comparisons*: If normality was met, a one-way ANOVA was used to compare classification accuracies across different models. If ANOVA produced a significant result ( $p < 0.05$ ), post-hoc pairwise comparisons were conducted using Tukey's Honest Significant Difference (HSD) test.

If normality was not met, the Kruskal-Wallis test was used as a non-parametric test to compare classification accuracies across models. If the Kruskal-Wallis test yielded a significant result ( $p < 0.05$ ), pairwise comparisons were conducted using Conover's post-hoc test with Bonferroni correction to control for Type I errors. To further interpret model differences, we computed Cliff's Delta for each pairwise comparison. Cliff's Delta quantifies the effect size of the difference between two distributions, indicating whether a difference is practically meaningful in addition to being statistically significant and provides insights into the relative performance of different models. A large effect size ( $|\delta| > 0.474$ ) indicates a strong

practical difference, whereas a small effect size ( $0.147 < |\delta| < 0.330$ ) suggests minor practical significance. Effect sizes close to zero indicate negligible differences.

### III. RESULTS

#### A. Data Preprocessing and Feature Selection

The dataset used in this study provided pre-extracted physiological features, as a result of preprocessing and feature selection, most participants (9 out of 10) retained 23 features, while one participant (UN\_105) retained 27 features. The four features removed for most participants were all related to EDA, specifically EDA\_Tonic\_SD, EDA\_Sympathetic, EDA\_SympatheticN, and EDA\_Autocorrelation.

#### B. EEG-Only ML Model Performance: Classification results for LR, MLP and SVM

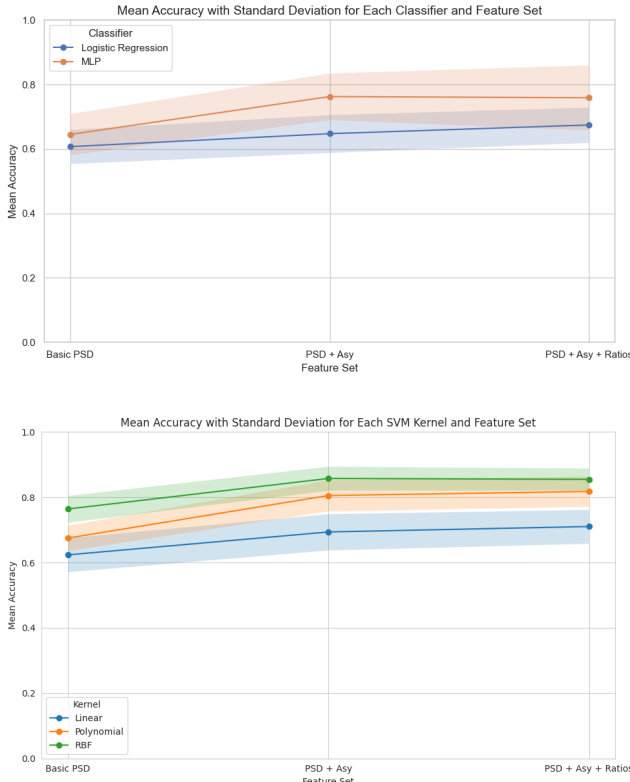


Fig. 3: Comparison of EEG-only classification performance for different machine learning models. Top plot: Logistic Regression and MLP across EEG feature sets. Bottom plot: SVMs with different kernels.

Figure 3 illustrates the classification performance of LR, MLP, and SVM across different EEG feature sets. MLP consistently outperformed LR, confirming that non-linear models benefit more from EEG-based cognitive load classification. With the Basic PSD feature set, LR achieved an accuracy of  $60.7\% \pm 5.3\%$ , while MLP performed slightly better at  $64.5\% \pm 6.5\%$ . Adding asymmetry features (PSD + Asy)

significantly improved both models, with LR reaching  $64.8\% \pm 8.6\%$  and MLP increasing to  $76.3\% \pm 7.3\%$ , marking the highest performance gain. However, adding power ratio features (PSD + Asy + Ratios) slightly improved LR ( $67.5\% \pm 5.5\%$ ) but caused a minor performance drop for MLP ( $75.9\% \pm 10.2\%$ ), possibly due to feature redundancy or increased feature dimensionality.

Linear SVM performed comparably to LR, achieving 69.4% accuracy on PSD + Asy features. However, non-linear kernels led to considerable improvements, with SVM Polynomial achieving 81.8% accuracy and RBF SVM reaching the highest performance of 85.6% using the same feature set. These results suggested that non-linear transformations in SVMs effectively capture cognitive load patterns in EEG data. Compared to MLP (76.3% accuracy on PSD + Asy), the RBF SVM exhibited superior performance, indicating that well-tuned non-linear kernels might generalize better than neural networks in this dataset.

#### C. Multimodal Model Performance

The classification results, summarized in Table I, demonstrated that incorporating multimodal data improved classification performance across all models.

Compared to the EEG-only models, multimodal LR accuracy increased from 67.5% (EEG) to 77.9%, while MLP performance improved from 76.3% (EEG) to 93.5%. This suggests that HRV, EDA, and TEMP signals indeed contribute to cognitive load classification.

Among SVM classifiers, SVM RBF (96.0%) and SVM Polynomial (94.0%) outperformed and SVM Linear (79.0%). The superior performance of RBF and Polynomial kernels confirmed that non-linear models benefited from the additional physiological signals.

Compared to previous literature, where LR achieved 71% accuracy using all participants, our multimodal models showed significant improvement, particularly in MLP and non-linear kernel methods SVM. This highlighted the effectiveness of multimodal feature fusion for cognitive load classification.

TABLE I: Performance comparison of various machine learning models using multimodal features.

Model	Accuracy	F1-Score	Precision	Recall
Literature LR	0.710	0.690	0.740	0.710
Our LR	0.778	0.777	0.785	0.771
MLP	0.934	0.935	0.935	0.936
SVM Linear	0.790	0.780	0.850	0.800
SVM Polynomial	0.940	0.940	0.970	0.940
SVM RBF	0.960	0.960	0.990	0.960

#### D. Spiking Neural Network Performance

As a result of the grid search, the optimal hybrid SNN model consisted of two fully connected layers without biases: the fc1 mapped the input features to a hidden representation (sized at 20 times the input dimension), and fc2 outputs a single neuron prediction. Both layers were followed by aCLIF neurons with  $\beta = 0.8$ , this value was tuned also by grid

search. Moreover, SNN models were trained using a batch size of 1, a learning rate of 0.001, and over 20 epochs. We employed stratified 5-fold cross-validation for each participant to select the best hyperparameter configuration based on mean validation accuracy.

As for the biologically inspired SNN, we used the same training process and network architecture except for the fc1 with a connection probability of 0.1. Also, a learnable beta parameter was incorporated within the leaky activation function. To transform continuous physiological features into spike representations, we applied LIF spike encoding ( $V_{\text{rest}} = 0.0$ ,  $V_{\text{reset}} = -65.0$ ,  $V_{\text{th}} = -50.0$ ,  $\tau = 29.0$ ,  $dt = 1$  ms,  $\text{num\_steps} = 40$ ).

Table II presents the performance of the SNN models trained for cognitive load classification. The hybrid SNN, which applied Adam optimization for fc1 and the Delta learning rule for fc2, achieved an accuracy of  $88.4\% \pm 3.5\%$ . This suggested that hybrid SNN architectures leveraging backpropagation could perform comparably to MLP (93.4% accuracy in Table I).

The bio-inspired SNN, which incorporated fc1 weight initialization from a normal distribution and a connection probability constraint ( $p_{\text{conn}}$ ), exhibited different performance trends based on input modality. When trained only on EEG features, accuracy dropped to  $73.7\% \pm 8.2\%$ . However, when multimodal features were integrated, performance increased to  $84.5\% \pm 11.0\%$  surpassing the baseline LR model. These results indicated that biologically constrained SNNs could benefit significantly from multimodal integration. Additionally, analysis of connection probability  $p_{\text{conn}}$  trends (see Fig. 4) suggested that lower connectivity enhanced classification accuracy, reinforcing the importance of sparsity constraints in neuromorphic learning.

TABLE II: Performance of Different SNN Architectures

SNN Model	Accuracy	F1 Score	Precision	Recall
Hybrid SNN	0.885	0.881	0.902	0.866
Bio-inspired SNN (EEG)	0.735	0.722	0.771	0.735
Bio-inspired SNN	0.843	0.835	0.881	0.844

#### E. Statistical Analysis of Model Performance

1) *Bootstrapping and Normality Test Results:* A Shapiro-Wilk test was conducted to assess normality of bootstrapped accuracy distributions for each model, revealing that most models followed a normal distribution, including the hybrid SNN ( $W = 0.998, p = 0.204$ ), the bio-inspired SNN trained with all modalities ( $W = 0.999, p = 0.957$ ), and the bio-inspired SNN trained on EEG only ( $W = 0.998, p = 0.491$ ). However, the SVM polynomial model ( $W = 0.997, p = 0.041$ ) exhibited a statistically significant deviation from normality ( $p < 0.05$ ). Due to this, we opted for a non-parametric Kruskal-Wallis test to assess differences in model accuracy.

2) *Kruskal-Wallis Test Results:* The Kruskal-Wallis test yielded a highly significant result ( $p < 0.0001$ ), indicating

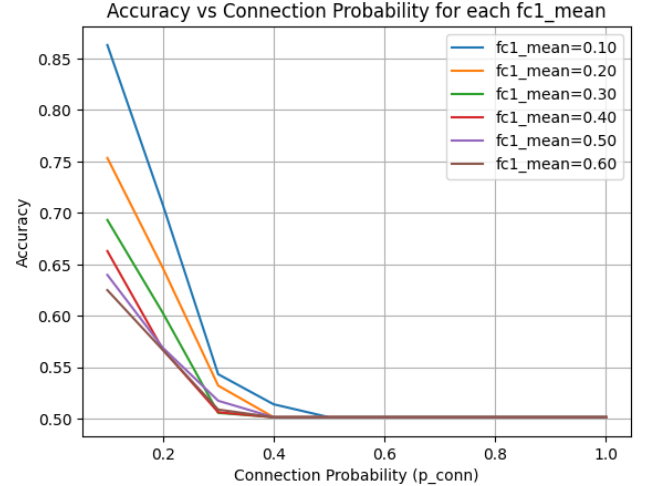


Fig. 4: Accuracy vs. Connection Probability ( $p_{\text{conn}}$ ) in Biologically Inspired SNN.

that at least one model significantly outperformed or underperformed relative to the others. To determine specific model differences, we conducted Conover's post-hoc analysis with Bonferroni correction.

3) *Post-hoc Analysis with Conover's Test and Cliff's Delta:* Table III presents the selected results of the pairwise Conover's test, including Bonferroni-corrected comparisons and Cliff's Delta effect sizes. All reported comparisons are statistically significant. Certain comparisons were omitted as they were not directly relevant to our research questions.

TABLE III: Selected conover's Test Post-hoc Comparisons with Bonferroni corrected values and Cliff's Delta ( $|\delta|$ )

Model 1	Model 2	Difference	$ \delta $
Literature LR	Our LR	-0.069	0.993
Literature LR	Hybrid SNN	-0.174	1.000
Literature LR	Bio-inspired SNN	-0.135	0.771
Our LR	Hybrid SNN	-0.105	0.997
Our LR	Bio-inspired SNN	-0.066	0.461
Hybrid SNN	Bio-inspired SNN	0.039	0.268
Bio-inspired SNN (EEG)	Bio-inspired SNN	-0.108	0.573
SVM RBF	Hybrid SNN	0.075	0.950
SVM RBF	Bio-inspired SNN	0.114	0.706

## IV. DISCUSSION

### A. Impact of Feature Selection and EEG-Based Models

The EEG-only models demonstrated that feature selection significantly impacts classification accuracy. The inclusion of asymmetry features (PSD + Asy) provided the highest accuracy gain, especially for non-linear models such as the MLP. However, adding power ratio features (PSD + Asy + Ratios) did not further enhance MLP performance, indicating that feature redundancy may have introduced noise rather than improving classification.

SVMs with non-linear kernels (Polynomial and RBF) outperformed LR and MLP on EEG-only features, achieving 85.6% accuracy with the RBF kernel. This suggested that EEG-based cognitive load classification benefited from non-linear transformations, which better captured complex neural activity patterns.

EEG-only classification results highlighted the impact of feature selection and non-linear modeling. Asymmetry features (PSD + Asy) significantly improved performance, while power ratio features had mixed effects, enhancing LR but slightly reducing MLP accuracy.

However, EEG alone remained insufficient for optimal classification, reinforcing the need for multimodal integration.

### B. Effectiveness of Multimodal Integration

Our results confirmed that multimodal feature fusion significantly enhanced classification performance. Compared to EEG-only models, incorporating HRV, EDA, and TEMP features improved model performance across all machine learning methods.

These findings indicated that physiological data from multiple modalities provided complementary information, reinforcing the need for multimodal integration in cognitive load assessment.

### C. Comparing Deep Learning and Neuromorphic Models

SNN models yielded interesting insights into neuromorphic approaches for cognitive load classification. The hybrid SNN, which leveraged backpropagation for fc1 and a Delta learning rule for fc2, achieved an accuracy of 88.4%, significantly higher than baseline LR model (77.8%) and SVM Linear (79.0%) with large effect size. This suggested that hybrid SNN architectures could perform better with simple ML models while maintaining biologically plausible learning dynamics. Moreover, the hybrid SNN showed higher accuracy than multimodal bio-inspired SNN though with a relatively small effect size ( $\Delta = 0.268$ ), indicating that their real-world performance remains comparable.

The bio-inspired SNN exhibited different performance trends based on input modality. When trained on EEG-only features, its accuracy dropped to 73.5%, reflecting the limited discriminative power of EEG under biologically constrained learning rules. However, when multimodal features were included, the bio-inspired SNN reached 84.3%. This reinforced the idea that biologically inspired architectures could benefit significantly from multimodal integration. Our SNN-based models exhibited higher accuracy variance (see Table IV) compared to traditional ML models, which demonstrated relatively lower accuracy fluctuations. This discrepancy arises from the fact that ML approaches underwent individualized hyperparameter tuning for each participant, whereas the SNN-based models were trained using a fixed set of hyperparameters without participant-specific optimization.

### D. Statistical Validation of Model Performance

Statistical analysis confirmed that the observed performance differences were significant. The Kruskal-Wallis test revealed

TABLE IV: Mean Accuracy and Standard Deviation of Different Models.

Model	Mean Accuracy	Standard Deviation
Literature LR	0.710	0.020
Our LR	0.778	0.015
MLP	0.934	0.017
SVM Linear	0.790	0.018
SVM Polynomial	0.940	0.016
SVM RBF	0.960	0.015
Hybrid SNN	0.885	0.034
Bio-inspired SNN (EEG)	0.735	0.079
Bio-inspired SNN	0.843	0.109

a significant effect of model type on classification accuracy ( $p < 0.0001$ ). However, practical post-hoc analysis showed that the significance varied depending on effect size and mean difference.

The multimodal bio-inspired SNN significantly outperformed its EEG-only variant, as indicated by a large effect size ( $|\delta| = 0.573$ ), confirming that incorporating multiple physiological signals significantly enhanced model performance and reinforced the benefits of multimodal fusion. Similarly, this model also showed medium-to-large effect sizes when compared to traditional machine learning models such as LR and SVM Linear, suggesting that neuromorphic models leveraging multimodal data could achieve superior accuracy compared to simpler ML approaches.

SVM RBF outperformed both the hybrid SNN (mean difference = 0.075,  $|\delta| = 0.950$ ) and bio-inspired SNN (mean difference = 0.114,  $|\delta| = 0.706$ ). These results suggested that well-tuned SVM RBF achieved better accuracy than neuromorphic approaches.

Furthermore, statistical analysis also confirmed that multimodal feature integration was essential for optimal performance in biologically inspired SNNs. When using only EEG data, performance significantly dropped. However, when additional physiological signals were incorporated, the bio-inspired SNN achieved much higher accuracy and was comparable to some well-tuned traditional ML models.

Overall, these findings highlighted that while neuromorphic models showed promising improvements over certain ML approaches, deep learning and well-optimized SVM models remained strong competitors in cognitive load classification tasks. These findings highlighted the potential of neuromorphic computing as an efficient alternative to traditional ML methods, particularly in real-time, low-latency, and low-power applications.

## V. CONCLUSION

Our findings highlight the importance of multimodal feature integration, non-linear classification, and biologically constrained neuromorphic computing for cognitive load classification. Future research should focus on optimizing SNN architectures for real-time, low-power applications by leveraging raw signals to identify novel biomarkers for cognitive

load detection and spike encoding. Additionally, exploring biologically inspired learning rules could enhance SNN performance, while neuromorphic hardware implementations should be investigated for real-time cognitive load monitoring.

## VI. ACKNOWLEDGEMENTS

We acknowledge the financial support of the Digital Society Initiative (DSI) at University of Zurich.

## REFERENCES

- [1] Miloš Pušica et al. “Mental workload classification and tasks detection in multitasking: Deep learning insights from EEG study”. In: *Brain Sciences* 14.2 (2024).
- [2] F. Dehais et al. “A neuroergonomics approach to mental workload, engagement and human performance”. In: *Frontiers in neuroscience* 14 (2020), p. 268.
- [3] G. Di Flumeri et al. “EEG-based mental workload neurometric to evaluate the impact of different traffic and road conditions in real driving settings”. In: *Frontiers in human neuroscience* 12 (2018), p. 509.
- [4] T. Kosch et al. “A survey on measuring cognitive workload in human-computer interaction”. In: *ACM Computing Surveys* 55.13s (2023), pp. 1–39.
- [5] L. Longo et al. “Experienced mental workload, perception of usability, their interaction and impact on task performance”. In: *PloS one* 13.8 (2018), e0199661.
- [6] J. Hassan et al. “EEG workload estimation and classification: a systematic review”. In: *Journal of Neural Engineering* (2024).
- [7] P. O’Connor et al. “Real-time classification and sensor fusion with a spiking deep belief network”. In: *Frontiers in neuroscience* 7 (2013), p. 178.
- [8] Yi Ding et al. “Measurement and identification of mental workload during simulated computer tasks with multimodal methods and machine learning”. In: *Ergonomics* 63.7 (2020), pp. 896–908.
- [9] C. Anders et al. “Unobtrusive measurement of cognitive load and physiological signals in uncontrolled environments”. In: *Scientific Data* 11 (2024), p. 1000.
- [10] E. Chicca, F. Stefanini, C. Bartolozzi, and G. Indiveri. “Neuromorphic electronic circuits for building autonomous cognitive systems”. In: *Proceedings of the IEEE* 102.9 (Sept. 2014), pp. 1367–1388. ISSN: 0018-9219.
- [11] Y. Liu et al. “Cognitive load prediction from multimodal physiological signals using multiview learning”. In: *IEEE Journal of Biomedical and Health Informatics* (2023).
- [12] F. et al. Bauer. In: *Biomedical Circuits and Systems, IEEE Transactions on* 13.6 (Dec. 2019), pp. 1575–1582.
- [13] Alessio Carpegna et al. “Neuromorphic Heart Rate Monitors: Neural State Machines for Monotonic Change Detection”. In: *2024 IEEE Biomedical Circuits and Systems Conference (BioCAS)*. IEEE, Oct. 2024.
- [14] De Luca et al. “A neuromorphic multi-scale approach for heart rate and state detection”. In: (2024).
- [15] E. et al. Donati. “Discrimination of EMG Signals Using a Neuromorphic Implementation of a Spiking Neural Network”. In: *Biomedical Circuits and Systems, IEEE Transactions on* 13.5 (2019), pp. 795–803.
- [16] Yongqiang Ma et al. “EMG-Based Gestures Classification Using a Mixed-Signal Neuromorphic Processing System”. In: *IEEE Journal on Emerging and Selected Topics in Circuits and Systems* 10.4 (2020), pp. 578–587.
- [17] Enea Ceolini et al. “Hand-gesture recognition based on EMG and event-based camera sensor fusion: a benchmark in neuromorphic computing.” In: *Frontiers in Neuroscience* 14 (2020).
- [18] M. et al. Sharifshazileh. “An electronic neuromorphic system for real-time detection of High Frequency Oscillations (HFOs) in intracranial EEG”. In: *Nature Communications* 12.1 (2021), pp. 1–14.
- [19] Olympia Gallou et al. “Online Epileptic Seizure Detection in Long-term iEEG Recordings Using Mixed-signal Neuromorphic Circuits”. In: *2024 IEEE Biomedical Circuits and Systems Conference (BioCAS)*. IEEE, Oct. 2024, pp. 1–5.
- [20] P.. Gong et al. “A Spiking Neural Network With Adaptive Graph Convolution and LSTM for EEG-Based Brain-Computer Interfaces”. In: *IEEE Transactions on Neural Systems and Rehabilitation Engineering* 31 (2023), pp. 1440–1450.
- [21] K. Kumarasinghe et al. “Brain-inspired spiking neural networks for decoding and understanding muscle activity and kinematics from electroencephalography signals during hand movements”. In: *Scientific Reports* 11 (2021), p. 2486.
- [22] K. et al. Burelo. “A Neuromorphic Spiking Neural Network Detects Epileptic High Frequency Oscillations in the Scalp EEG”. In: *Scientific Reports* 12.1 (2022), p. 1798.
- [23] Y. Hadad et al. “Situational Awareness Classification Based on EEG Signals and Spiking Neural Network”. In: *Applied Sciences* 14.19 (2024), p. 8911.
- [24] Z. Yan et al. “EEG classification with spiking neural network: smaller, better, more energy efficient”. In: *Smart Health* 24 (2022), p. 100261.
- [25] Jason K Eshraghian et al. “Training spiking neural networks using lessons from deep learning”. In: *Proceedings of the IEEE* 111.9 (2023), pp. 1016–1054.